Research Article

Nano Biomed Eng

Surface Modification of Mesoporous Silica Nanoparticles with Hexamethyl Disilazane as Smart Carriers for Tocopherol Acetate

Ayesha Shiekh[1], Ayesha Mushtaq[1], Uzma Jabeen[1], Farrukh Bashir[1], Manzar Zahra[2], Farida Behlil[1], Nayab Hina[1], Irfan Hafeez[3]

[1]Department of Chemistry, Sardar Bahadur Khan Women's University, Quetta, Pakistan
[2]Department of Chemistry, Lahore Garrison University, Lahore, Pakistan
[3]PCSIR Laboratories, Lahore, Pakistan

Corresponding author. E-mail: ayeshamushtaq2000@yahoo.com

Received: Aug. 26, 2022; **Revised:** Oct. 15, 2022; **Accepted:** Nov. 14, 2022; **Published:** Nov. 30, 2022

Citation: A. Shiekh, A. Mushtaq, U. Jabeen, et al. Surface modification of mesoporous silica nanoparticles with hexamethyl disilazane as smart carriers for tocopherol acetate. *Nano Biomedicine and Engineering*, 2022, 14(3): 216–224.

DOI: 10.5101/nbe.v14i3.p216–224

Abstract

Nowadays, nanotechnology is growing very fast, appearing every day in many fields related to this nanotechnology. In the present study silica nanoparticles (Si NPs) were synthesized, their surface was modified using a silazane and mesoporous Si NPs were further used for the loading tocopherol acetate. Si NPs were synthesized from tetraethyl orthosilicate (TEOS) in the presence of NaOH, with an easily handled, well known Stober method. In this, procedure TEOS was used as a source of silica and treated with NaOH and H_2O, undergoing condensation and hydrolysis reactions to produce Si NPs. These Si NPs were then modified by the hexamethyl silazane to avoid agglomeration and can be used easily for targeted delivery, as smart carriers. In the end, tocopherol acetate was successfully loaded in the modified Si NPs and different parameters were recorded for optimum loading. All the samples were characterized through SEM XRD, FTIR, BET and UV-VIS spectroscopy. XRD peaks reveled the typical peak of mesoporous Si NPs appeared at $2\theta = 22°$. The pore size was found to be 2.45 nm. BET surface area was found to be 694.29 m^2/g. FTIR presented the main peaks of functional groups at 1600 cm^{-1}, 1000 cm^{-1} and 2900 cm^{-1} respectively. Modified Si NPs were synthesized and characterized, and the tocopherol was loaded inside the mesoporous Si NPs successfully. These experiments showed that mesoporous Si NPs can be used as smart carriers to deliver broad types of drugs efficiently.

Keywords: Silica nanoparticles; Silazane; Drug delivery; Mesoporous

Introduction

In the 2000s, researchers showed great interest towards silica nanoparticles (Si NPs) due to its unusual properties which recommended their applications in chromatographic separation, catalysis, molecules adsorption, etc [1]. In 2001, silica was introduced as new Mesoporous Crystalline Material (MCM-41) and mesoporous silica nanoparticles (MSNs) with its: excellent compatibility, well-organized pore size properties, deep pore size distribution, large pore volume for drug accommodation and high surface area. Si NPs are highly biocompatible due to presence of abundant silanol groups on their surface and therefore, silica-based nanomaterials are getting popularity in biomedical applications. The silanol groups are

involved in the post-synthesis functionalization of the silica, can modify the interaction between host and guest molecule's delivery, and produced it in constant and controllable manners, particularly, when used as drug carriers [2].

It has been explored that MSNs are getting attraction due to their biomedical applications. Mesoporous silica nanomaterials became famous due to their promising nature to overcome all the problems related to targeted delivery and producing sustained and controlled release of a drug. Nanomaterials are extensively used as drug delivering agent, due to their favorable chemical properties, biocompatibility and thermal stability. At advanced level, employing MSNs was also studied in the blood vessels to check the behavior of nanoparticles. This research established the size and surface possession on the interface of MSNs with human red blood cell membranes and suggested that the appropriate surface modification of nanomaterials can enhance their biocompatibility and reduce their dangerous effects on red blood cells. The actual unique advantage of Si NPs is the smart delivery, outstanding biocompatibility, good hydrophobicity, systemic stability and resistance to pH changes with good multi-functionality. They are smart carriers, as they can permeate easily through the tumor tissues (active or passive targeting) because of their nano size and releasing the drug in a continuous manner. Popularity of silica nanomaterials as a smart nano carrier and normal drug vehicle is increasing because of their prominent and irregular mesoporous structure [2].

Takeuchi et al. prepared polypropylene grafted silicon dioxide (PP-g-SiO_2) nanoparticles by reacting SiO_2 with hydroxylated PP (PP-OH) situated on terminals. The synthesized polypropylene-silica nanocomposite with great uniform dispersed phase was obtained by using sol-gel method of silicon alkoxide [3].

Silanol (hydroxyl groups) that are present on mesoporous silica nanoparticles, react as very suitable and secure points of organic functionalization. To present certain organic groups, mainly post synthesis method has been introduced onto the surface of silanol on a variety of collected silica materials. Generally, precursors such as organochlorosilanes or organoalkoxysilanes are used for surface functionalization, which is active to functionalize the surface of mesoporous silica nanoparticles [4]. Two reaction methods are used to synthesized MSNs, and the most common is under basic conditions through hydrolysis and condensation process of silicon sources, called as the Stober method [5].

These mesoporous nanomaterials are used in different analytical fields, target delivery system, bio-sensing, cellular uptake, bio-medicines, etc. The MSNs own a definite framework with bigger surface area, as well as their porous structure allows different functional groups to attach with specific targeted site. Chemically, the mesoporous carriers have active site surfaces and structure like honeycomb. Functionalization is enabled by active surfaces to link therapeutic molecules.

To determine the association of Mesoporous Crystalline Material (MCM) and their loading capability and pore size, different MSNs with pore sized (4–25 nm) were made using two surfactants cetyl-trimethyl ammonium bromide (CTAB) and cetyl-trimethyl ammonium tosylate (CTAT). Recrystallization facile vacuum pump process was used to encapsulate the tocopherol acetate. The drug loading dimensions, and enclosed competences of modified nano carrier were investigated and compared with pure MSNs in different pH conditions. Antioxidant properties, cytotoxicity and hemolysis were also observed for mesoporous drug delivery for the assurance of its bioactivity [6].

Si NPs and other sources of silicon have been applied and found significant to mitigate the adverse effect of salt stress in wheat [7–10]. However, in biomedical fields, SiNPs can be used as smart nanocarriers. For drug delivery options, biodegradable porous silicon particles under development for drug delivery with optimum particle size can be used as smart nanocarriers. The particle size depends upon medical use, and microparticles can perform specific illustrations as smart carriers [11].

MSNs are getting popular in modern medicine applications, due to their applications as nano carriers for drug delivery and as well as for their non-toxicity. The invitro cytotoxicity test was done by MTT assay (3-(4,5-dimethylthiazol-2-yl)-2,5-diphenyltetrazolium bromide) for breast cancer cell assessment, the commonly used MCF (cell lines), which showed that silica nanoparticles are safe drug agents [12]. It has been reported that SiNPs are nontoxic and reach to their target point safely without affecting healthy tissues [13]. Si NPs interact with immunocompetent cells and induce immune toxicity. However, the toxic

effects of Si NPs on the immune system have been inadequately reviewed [14].

In this research, our key objective is synthesizing the monodispersed, spherical, hexamethyl disilazane-capped Si NPs which can be used in several biological fields. The fundamental MSNS were synthesized from tetraethyl orthosilicate (TEOS) according to the advanced Stober process, and these MSNs were used as smart carriers by loading tocopherol.

Materials and Methods

TEOS was purchased from Sigma Aldrich. Analar grade chemicals such as ethanol, methanol, cetyl trimethylammonium bromide, benzyl tri-N-butyl bromide, sodium dodecyl benzene sulphonate, hexamethyl disilazane, α-Tocopherol, and toluene (solvent) were also purchased. Figure 1 shows the schematic representation for the Si NPs synthesis, modification, loading and optimization of tocopherol and their characterization.

Synthesis of silica nanoparticles

SiNPs were synthesized by well-known Stober method. At first, deionized water (120 mL) and 1 mol/L NaOH (1.75 mL) was taken in a beaker with CTAB (0.5 g), heated for 1h at 80 °C with constant stirring at 100 r/min till the solution become clear, then its pH was maintained at 12. Then TEOS was added to this solution with constant stirring and white precipitate were observed after 3 min. Leave the mixture stirring for some time then centrifuge for 15 min. Wash it 3 times with excess water and ethanol solution (3:4), and then after calcination, it was dried in oven at 120 °C for 8 h. Grayish color indicated the formation of the SiO_2 NPs. Fine particle size can be obtained by prolonged sonication [15]. Then Si NPs were characterized by ultra violet visible infrared spectroscopy (UV-VIS) and Fourier transform infrared spectroscopy (FTIR).

Three different surfactants were used to get various porous medium and surface diameter. Sodium dodecyl benzene sulphonate (0.4 g), benzyl tri-N-butyl bromide (0.8 g), cetyltrimethylammonium bromide (0.5 g) were used to prepare SiNPs. Different surfactants, sodium dodecyl benzene (SDBS), benzyl tri-N-butyl bromide and CTAB were used to obtain Si NPs with different pore sizes [16–19]. The best results were achieved using CTAB in this experiment.

Modification of MSNs by hexamethyl disilazane

Silica surface modification (functionalization) and all handlings were performed in two neck isopiestic flasks. Freshly dried silica (1 g) was mixed with toluene (25 mL). In this mixture, Hexamethyl disilazane (3 mL) and hydrochloric acid were poured, maintaining the temperature at 100–150 °C. This reaction was kept for 3–4 h. It was centrifuged and washed with solvent (ethanol) for multiple times and kept for drying under oven at 110 °C.

Calibration curve for tocopherol

A UV-VIS spectrophotometer (Shimadzu 1700) was used. The drug tocopherol acetate (vitamin E) commercially available was used due to its ease and availability. Stock solution was prepared from the drug tocopherol acetate (1 mg/L) and further dilutions were made as 5 mg/L, 10 mg/L, 15 mg/L, 20 mg/L, 25 mg/L, and 50 mg/L. Solvent such as methanol or acetonitrile was used as a reference opposite to the standard solution of tocopherol acetate. Lambda max of tocopherol used was 284 nm. Tocopherol acetate 5 mg/L solution with 10% ethanolic solution was used for loading tocopherol. First calibration curve was taken before loading tocopherol and it was observed that 5 mg/L solution led to load tocopherol easily because above 5–10 mg/L, there remained its solubility issue.

Loading tocopherol in MSNs

A mixture of 5 mg/L tocopherol acetate and 50 mg of dried Si NPs was soaked into the 10% ethanol solution, in a beaker and kept on stirring for about 12 h. After tocopherol loading process, the solution was centrifuged, and the supernatant was used to

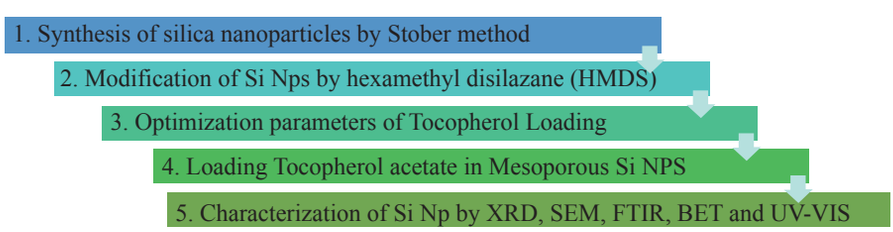

Fig. 1 The schematic representation for the Si NPs synthesis to characterization

check the results. Different parameters were taken to identify the optimization of tocopherol loading. All the parameters were performed consistently and gained the optimization rate. All the parameters were performed with same factors using the dose which was already optimized at rate of 5 mg/L.

Table 1 indicates pH, time, adsorbent and temperature study for loading of tocopherol acetate as well as dosage parameters for loading tocopherol acetate.

Results and Discussion

In the present study, SiNPs were synthesized by breakdown of TEOS in the first step. In the second step, the synthesized SiNPs were surface, modified by HMDS. In the last step, tocopherol acetate was loaded inside the MSNs at optimum conditions. A pH = 9 optimum tocopherol was loaded in 12 h at 22 °C. The optimum concentration found 5 mg/L for loading tocopherol. Scanning electron microscopy (SEM) images of the prepared Si NPs showed that particles were spherical in nature. Three samples with different surfactants (cetyltrimethylammonium bromide, sodium dodecylbenzene sulphonate, and benzyl trimethyl ammonium) with help of SEM were analyzed (Fig. 2).

The structure of prepared silica nanoparticles was recorded by X-ray diffraction (XRD) by powder diffractometer using Cu-Kα = 1.54 Å (1 Å = 0.1 nm) with a scanning rate of 2θ/min (Fig. 3). The XRD spectra of Si NPs appeared as a broad hollow peak centered at two theta value of 22°. This XRD pattern corresponds to pair distubition function analysis (PDF) card standard for silica-cristobalite phase JCPDS # 00-001-0424 that confirmed amorphous nature of SiNPs (Fig. 3), which is similar to previously reported studies [20, 21].

Nitrogen adsorption/desorption analysis

Nitrogen adsorption/desorption isotherms were measured at 77.35 K by using micromeritics Gemini

Table 1 Effect of different parameters on Tocopherol loading

1	pH for tocopherol	Dose and time	Concentration of drug & temperature	Temperature and speed
A	pH = 3	50 mg 3 h	5 mg/L at 22 °C	10 mL 20 r/min
B	pH = 9	50 mg 3 h	5 mg/L at 22 °C	10 mL 20 r/min
C	pH = 12	50 mg 3 h	5 mg/L at 22 °C	10 mL 20 r/min
2	Time for loading	Mass and volume	Concentration of drug	Speed and temperature
A	3 h	50 mg 10 mL	5 mg/L	20 r/min 22 °C
B	9 h	50 mg 10 mL	5 mg/L	20 r/min 22 °C
C	12 h	50 mg 10 mL	5 mg/L	20 r/min 22 °C
3	Amount of Si NPs	Volume and time	Concentration of drug & pH	Speed and temperature
A	5 mg	10 mL 12 h	5 mg/L at pH = 9	20 r/min 22 °C
B	25 mg	10 mL 12 h	5 mg/L at pH = 9	20 r/min 22 °C
C	50 mg	10 mL 12 h	5 mg/L at pH = 9	20 r/min 22 °C
4	Dose of drug	Adsorbent mass and volume	Time and pH scale	Speed and temperature
A	2 mg/L	50 mg/10 mL	12 h at pH = 9	20 r/min 22 °C
B	5 mg/L	50 mg/10 mL	12 h at pH = 9	20 r/min 22 °C
C	10 mg/L	50 mg/10 mL	12 h at pH = 9	20 r/min 22 °C
5	Temperature	Dose and volume	Drug Concentration	Speed and time
A	22 °C	50 mg/10 mL	5 mg/L	20 r/min 12 h
B	80 °C	50 mg/10 mL	5 mg/L	20 r/min 12 h
C	100 °C	50 mg/10 mL	5 mg/L	20 r/min 12 h

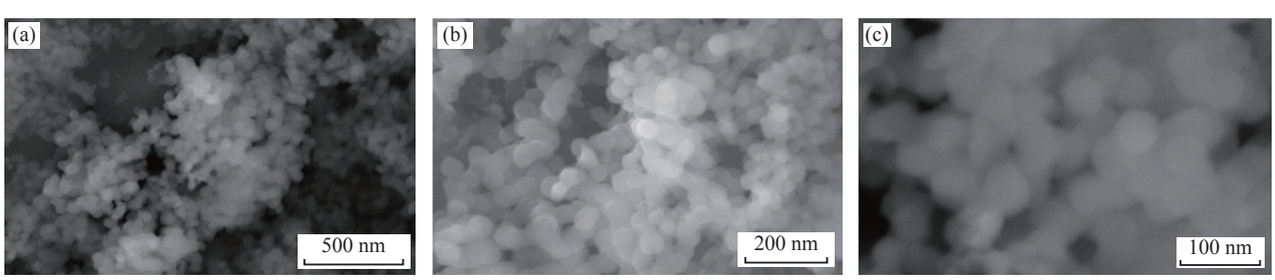

Fig. 2 SEM of CTAB surfactant showed Si NPs at resolution of **(a)** 500 nm, **(b)** 200 nm and **(c)** 100 nm

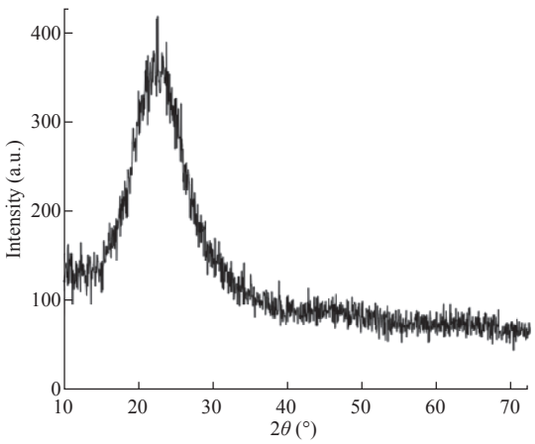

Fig. 3 XRD pattern of prepared silica nanoparticles

VII 3.03 system. On a vacuum line it was degassed at 746 K. The porous size division curve was derived from the adsorption branch of isotherm using Barret-Joyner-Halanda (BJH) method. Calculation of specific surface area by utilizing Brunauer-Emmet-Teller (BET), 0.25 was maximum relative pressure (P/P_0) 0.25, was concluded from total adsorbed pore volume. BET surface area was 694.2918 m^2/g, cumulative pore volume was 0.278503 cm^3/g, and average pore size 2.4507 nm.

Figure 4(a) indicates the relationship between relative pressure and quantity adsorbed (cm^2/g) in the pore. The maximum pore volume achieved

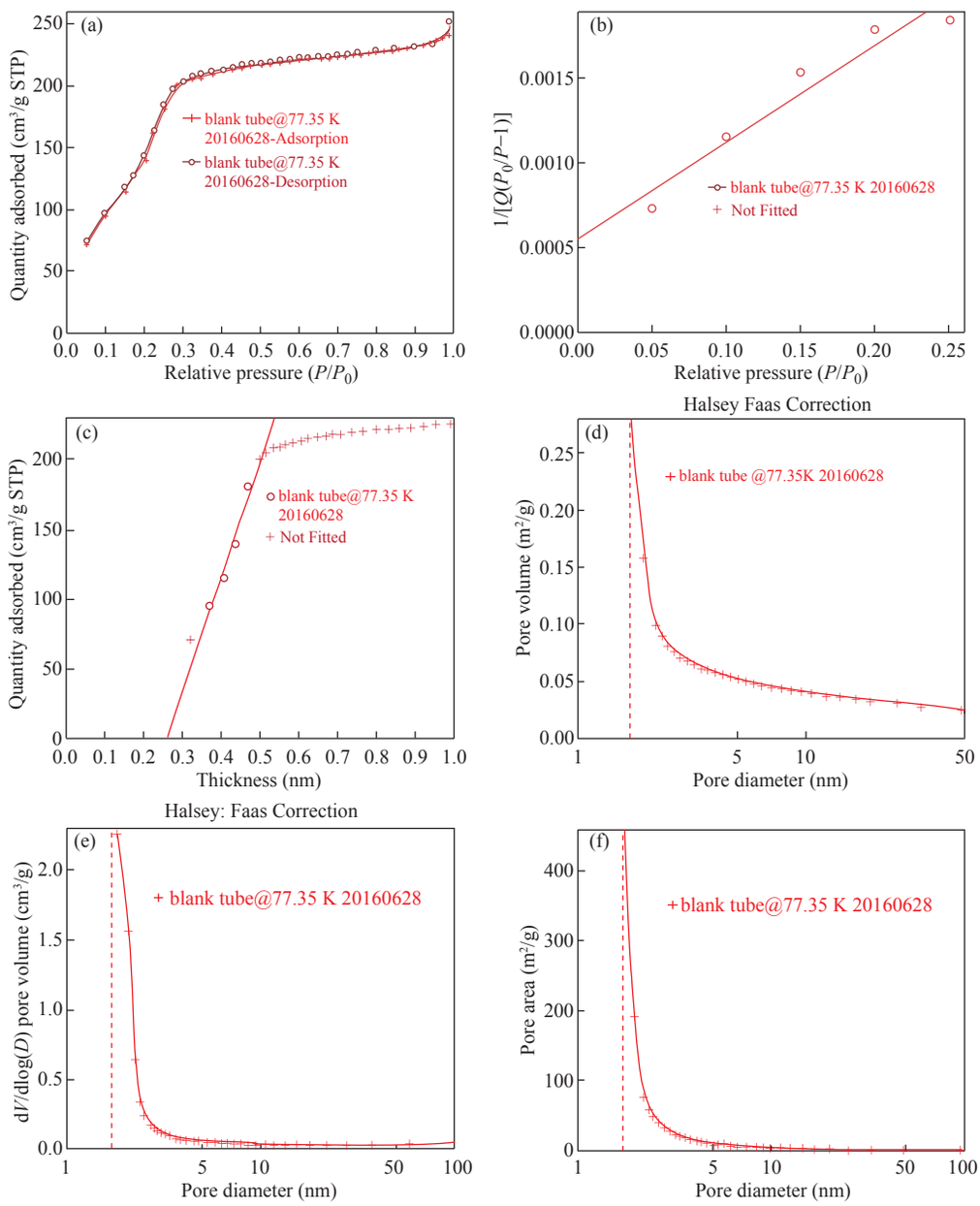

Fig. 4 (a) Isotherm linear plot of nanoparticles, **(b)** BET surface area of nanoparticle, **(c)** Toco plot of silica nanoparticles, **(d)** BJH adsorption cumulative pore volume of sample, **(e)** Pore volume of silica nanoparticles, **(f)** Larger porous volume of silica nanoparticles

at 200 cm²/g quantitative adsorbent at P/P_0 = 0.3, and constantly increased to 240 cm²/g at P/P_0= 0.9 relative pressure. Figure 4(b) showed surface area of nanoparticle. This calibrated graph was the plot of relative pressure against quantitative pressure which was increasing from 0.0005 to 0.0020 (relative pressure). A calibrated graph (Fig. 4(c)) for the thickness of pore present in the Si NPs indicated the relation between thickness and quantity absorbed, and the pore thickness was increased from 100 cm² to 180 cm². BTH is a technique in which powdered sample is analyzed to check the pore diameter. Figure 4(d) indicated a high porous volume of 0.26 cm/g. Figure 4(e) represented the pore diameter of Si NPs against pore volume. The cumulative pore volume was 0.278503 cm³/g, and the average pore size was 2.4507 nm. Figure 4(f) is the pore volume against the pore area. It highlighted the lager porous Si NPs with larger pore area. Overall pore volume of Si NPs was 0.278503 cm³/g, and their average pore size was 2.4507 nm.

FTIR analysis

The simple SiNPs synthesized in 1st step are SA-1, whereas SiNPs were modified by HMDS in 2nd step (SA-H). The characteristic peaks of SA-1 were 1365 cm^{-1}, 1645 cm^{-1}, and 3268 cm^{-1}. The peaks observed at 1046 cm^{-1} and 1060 cm^{-1} in both spectra were due to Si-O-Si stretch, whereas in SA-H, the peak appeared at 1625 cm^{-1}, 1633 cm^{-1}, 757 cm^{-1}, and 3375 cm^{-1}. The peak appeared at 970 cm and 802 cm^{-1} were due to Si-O-Si stretching and bending in-plane bending vibration respectively [22]. The peak observed in both spectra in the region of 790–806 cm^{-1} was due to the presence of quartz in silica. The above all peaks were similar in both unmodified and modified silica except the peaks observed at 2922 cm^{-1} and 2852 cm^{-1} due to sp^3 C-H stretch, 1467 cm^{-1} and 1366 cm^{-1} due to CH_2 and CH_3 bending vibration, which are absent in unmodified silica that confirmed the modification of silica with HDMS. These all peaks confirmed the formation of modified silica with HMDS (Fig. 5).

Loading tocopherol in silica nanoparticles

Different standard solutions were made by the drug tocopherol and analyzed by UV-VIS spectroscopy. The lowest absorption peak shown by the solution was 5 mg/L and intense absorption peak was showed by 50 ppm solution (Fig. 6).

Passive methodology was proposed to load the drug in the Si NPs. Three various solvents were used to load drug molecules. 5 mg/L drug, and 50 mg carrier and 10% polar solvent (methanol, ethanol,

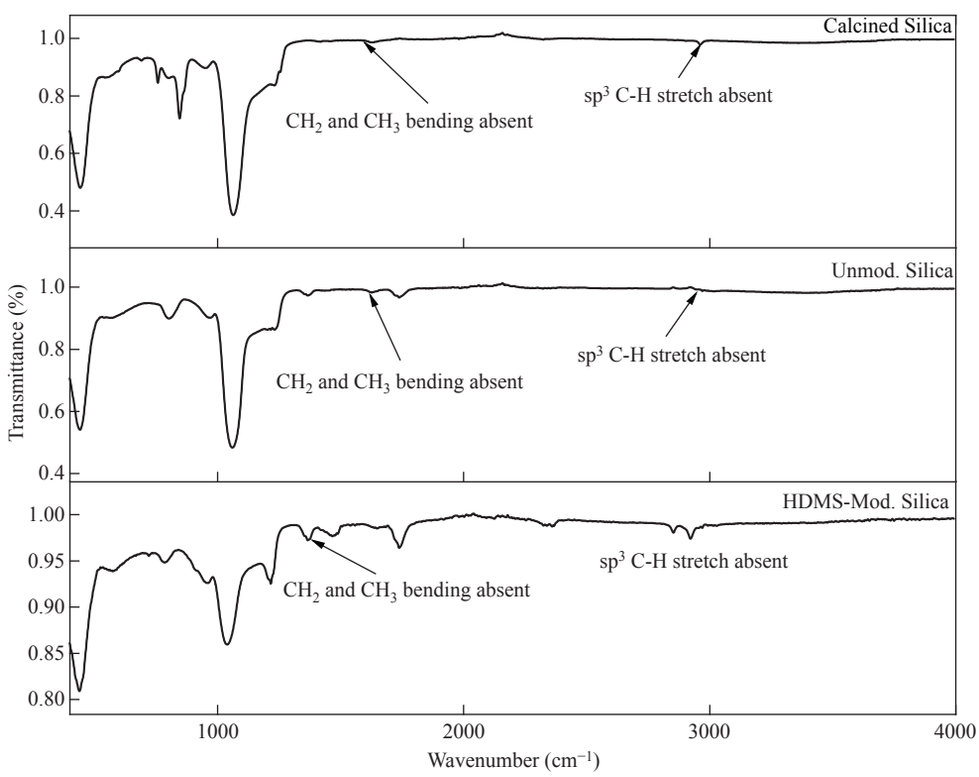

Fig. 5 (a) FTIR of calcined, **(b)** Unmodified, **(c)** HMDS Si NPs

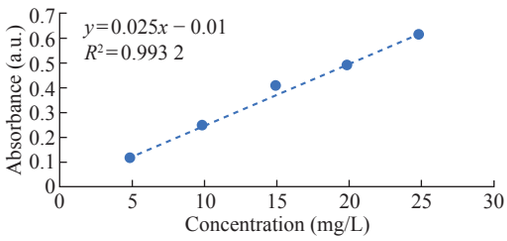

Fig. 6 Calibration curve of tocopherol in 10% ethanol solution

and acetonitrile) The suspension was then kept for stirring overnight. The effects of temperature and loading time was observed sharply. The tocopherol loaded Si NPS were then collected and centrifuged (3000 r/min) and the supernatant was progressed for UV-VIS spectrophotometry. Both modified and unmodified adsorbents were kept under loading process. In a few cases both the polar solvents become hindered and the solvents are responsible for the drug entrapment. Low polar solvents are less capable for drug loading, while the research concluded that methanol and acetonitrile had high entrapment efficiency. Different parameters were given by the loading process. The appropriate temperature for the loading was 25 °C and the time for the maximum loading was 12 h, while 50 mg concentration of drug carrier and 5 mg/L drug loading was optimized. Keeping all these factors constant, 51% of the entrapment according to these above-mentioned factors was completed.

In this study three surfactants such as sodium dodecyl sulfate (SDS), sodium dodecyl benzenesulfonate (SDBS), and cetyltrimethylammonium bromide (CTAB) were used for Si NPs. Best results were achieved by CTAB in our study, with ideal pore size. The pore diameter was 50 nm, which is in agreement to prior studies [16-18]. The reaction was processed in basic or alkaline conditions because presence of ammonium ions in the reaction medium have a twofold role: first it alters the pH of the medium, and second it reduces the amount of the energy required to start the nucleation, or in other words, enhance the rate of nucleation [23].

The content of the surfactant showed vital consequences in the structure distribution of nanospheres [22, 24]. Different kinds of surfactants were used in this study to make a variety of MSNs with different pore sizes and different shapes. SEM results showed that, addition of CTAB produced the sample of 0.27 cm^3/g pore volume, surface area 694 m^2/g, and 2.45 nm pore size; then further, the size of the particle raised more due to increase in reaction time and at the last no change appeared. The particle size decreased by reducing the concentration of NH_3 and TEOS, and increased with increment of same chemicals [4, 18]. The Si NPs could be synthesized under 80 °C, and above this temperature, nanoparticles are smashed. The unmodified Si NPS lonely couldn't emulsify while the HMDS modified Si NPs material form stable emulsion added with discrete droplets with little water hindrance.

HMDS was used to modify hydrophilic silica to be hydrophobic and to reduce the agglomeration [25]. Another main purpose was also to make sure that when the HMDS modified silica (hydrophobic silica) reached the targeted site it released at once instead it released beyond the delivery point [26, 27].

The initial characterization was done by UV-VIS spectrophotometer. The suggested UV spectrophotometric technique showed exciting features such as swiftness, easiness, and less expensive, and did not contained cultured or costly instrumentation. The method is proposed for standard serial dilutions commonly [24]. In another study, comparison of qualitative with optimized quantitative approach for UV/VIS spectroscopic identification of tocopherol was done [2].

In this research, we created innovative strategy to manufacture a new type of mesoporous silica contexts for delivery of water insoluble drug Vitamin E. These Si NPs can also be used as smart carriers for any drug efficiently by increasing their bioavailability and dispersity at target point. Average pore size of drug delivery agent was 2.4 nm. In the meantime, similar results were achieved. The frame-up of the unbalanced tocopherol exclusive in the amino imbedded mesoporous network might progress drug stability and avoid pharmacological deficiency when exposed in to air for 48 h [6].

According to the SEM results, the size of nanoparticles ranged between 100 nm to 500 nm, which is acceptable for any drug loading and drug releasements according to references [3, 17]. In XRD results, the peak appeared at $2\theta = 22°$, showing the crystalline structure of Si NPs. In FTIR, the characteristics peaks were found at 2922 cm^{-1}, 2856 cm^{-1}, 1356 cm^{-1} and 1467 cm^{-1} respectively [28, 29]. The BET, surface area was 694.2918 m^2/g, which is in agreement with other studies [26].

If the drug (entrapment) loading is 60% then drug releasement may be 41% because some of the drug

trapped in inner pore volume and may not be release to the targeted point [22, 30, 31]. Different parameters were also checked for the optimization levels of drug loading, therefore, the highest rate of drug loading, was found at optimized conditions. The optimum conditions can be further used for the loading of tocopherol or other drugs also.

Conclusion

Stober method is the simplest method for preparation of silica nanoparticles. Mesoporous silica nanoparticles are gaining attention in biomedicine as they can be used for loading any drug inside these nano-carriers. In this study, tocopherol acetate was successfully loaded in the modified Si NPs and different parameters were recorded for optimum loading. The pore size was found to be 2.45 nm, and BET surface area was 694.29 m^2/g. Modified Si NPs were synthesized and characterized using different techniques. The present study concluded that mesoporous silica nanoparticles can be used as nano-carriers to load and deliver broad types of drugs efficiently.

Acknowledgments

Authors would like to thank Higher Education Commission of Pakistan and SBK Women's University for their valued research funding. The authors would like to thank the Department of Chemistry, Quaid-i-Azam University, Islamabad for providing lab facilities.

Conflict of Interests

The authors declare that no conflict of interest exists.

References

[1] M. Su. Synthesis of highly monodisperse silica nanoparticles in the microreactor system. *Korean Journal of Chemical Engineering*, 2017, 34: 484–494. https://doi.org/10.1007/s11814-016-0297-x

[2] M. Vallet-Regí, M. Colilla, I Izquierdo-Barba, et al. Mesoporous silica nanoparticles for drug delivery: Current insights. *Molecules*, 2017, 23: 47. https://doi.org/10.3390/molecules23010047

[3] K. Takeuchi, M. Terano, T. Taniike. Sol–gel synthesis of nano-sized silica in confined amorphous space of polypropylene: Impact of nano-level structures of silica on physical properties of resultant nanocomposites. *Polymer*, 2014, 55: 1940–1947. https://doi.org/10.1016/j.polymer.2014.03.003

[4] X.L. Ji, Q.Y. Hu, J.E. Hampsey, et al. Synthesis and characterization of functionalized mesoporous silica by aerosol-assisted self-assembly. *Chemistry of Materials*, 2006, 18: 2265–2274. https://doi.org/10.1021/cm052764p

[5] E.D. Mohamed Isa, H. Ahmad, M.B. Abdul Rahman. Optimization of synthesis parameters of mesoporous silica nanoparticles based on ionic liquid by experimental design and its application as a drug delivery agent. *Journal of Nanomaterials*, 2019, 2019: 1–8. https://doi.org/10.1155/2019/4982054

[6] Z.X. Mai, J.L. Chen, Y. Hu, et al. Novel functional mesoporous silica nanoparticles loaded with Vitamin E acetate as smart platforms for pH responsive delivery with high bioactivity. *Journal of Colloid and Interface Science*, 2017, 508: 184–195. https://doi.org/10.1016/j.jcis.2017.07.027

[7] T. Kousar, N. Sabir, A. Mushtaq, et al. Influence of silica gel on ion homeostasis in salt stressed wheat varieties of balochistan. *Silicon*, 2021, 13: 4133–4138. https://doi.org/10.1007/s12633-020-00706-9

[8] A. Mushtaq, S. Rizwan, N. Jamil, et al. Influence of silicon sources and controlled release fertilizer on the growth of wheat cultivars of Balochistan under salt stress. *Pakistan Journal of Botany*, 2019, 51: 1561–1567. https://doi.org/10.30848/pjb2019-5(44)

[9] A. Mushtaq, N. Sabir, T. Kousar, et al. Effect of sodium silicate and salicylic acid on sodium and potassium ratio in wheat (*Triticum aestivum L.*) grown under salt stress. *Silicon*, 2022, 14: 5595–5600. https://doi.org/10.1007/s12633-021-01342-7

[10] A. Mushtaq, Z. Khan, S. Khan, et al. Effect of silicon on antioxidant enzymes of wheat (*Triticum aestivum L.*) grown under salt stress.*Silicon*, 2020, 12: 2783–2788. https://doi.org/10.1007/s12633-020-00524-z

[11] E. Nekovic, C.J. Storey, A. Kaplan, et al. A gentle sedimentation process for size-selecting porous silicon microparticles to be used for drug delivery via fine gauge needle administration. *Silicon*, 2022, 14: 589–596. https://doi.org/10.1007/s12633-020-00895-3

[12] S. Rasouli, S. Davaran, F. Rasouli, et al. Positively charged functionalized silica nanoparticles as nontoxic carriers for triggered anticancer drug release. *Designed Monomers and Polymers*, 2014, 17: 227–237. https://doi.org/10.1080/15685551.2013.840475

[13] M. Vallet-Regí. Our contributions to applications of mesoporous silica nanoparticles. *Acta Biomaterialia*, 2022, 137: 44–52. https://doi.org/10.1016/j.actbio.2021.10.011

[14] L.J. Chen, J. Liu, Y.L. Zhang, et al. The toxicity of silica nanoparticles to the immune system. *Nanomedicine*, 2018, 13: 1939–1962. https://doi.org/10.2217/nnm-2018-0076

[15] A. Mushtaq, N. Jamil, M. Riaz, et al. Synthesis of Silica Nanoparticles and their effect on priming of wheat (*Triticum aestivum L.*) under salinity stress. *Biological Forum*, 2017, 9: 150–157.

[16] A. Liberman, N. Mendez, W.C. Trogler, et al. Synthesis and surface functionalization of silica nanoparticles for nanomedicine.*Surface Science Reports*, 2014, 69: 132–158. https://doi.org/10.1016/j.surfrep.2014.07.001

[17] N. Debnath, S. Mitra, S. Das, et al. Synthesis of surface functionalized silica nanoparticles and their use as entomotoxic nanocides. *Powder Technology*, 2012, 221: 252–256. https://doi.org/10.1016/j.powtec.2012.01.009

[18] Q.S. Huo, D.I. Margolese, G.D. Stucky. Surfactant control of phases in the synthesis of mesoporous silica-based materials. *Chemistry of Materials*, 1996, 8: 1147–1160. https://doi.org/10.1021/cm960137h

[19] P. Velmurugan, J. Shim, K.J. Lee, et al. Extraction, characterization, and catalytic potential of amorphous silica from corn cobs by Sol-gel method. *Journal of Industrial and Engineering Chemistry*, 2015, 29: 298–

303. https://doi.org/10.1016/j.jiec.2015.04.009
[20] B. Purnawira, H. Purwaningsih, Y. Ervianto, et al. Synthesis and characterization of mesoporous silica nanoparticles (MSNp) MCM 41 from natural waste rice husk. *IOP Conference Series*: *Materials Science and Engineering*, 2019, 541: 012018. https://doi.org/10.1088/1757-899X/541/1/012018
[21] E. Herth, R. Zeggari, J.Y. Rauch, et al. Investigation of amorphous SiO_x layer on gold surface for Surface Plasmon Resonance measurements. *Microelectronic Engineering*, 2016, 163: 43–48. https://doi.org/10.1016/j.mee.2016.04.014
[22] Q.C. Guo, R. Ghadiri, T. Weigel, et al. Comparison of *in situ* and *ex situ* methods for synthesis of two-photon polymerization polymer nanocomposites. *Polymers*, 2014, 6: 2037–2050. https://doi.org/10.3390/polym6072037
[23] M. Mohseni, K. Gilani, S.A. Mortazavi. Preparation and characterization of rifampin loaded mesoporous silica nanoparticles as a potential system for pulmonary drug delivery. *Iranian Journal of Pharmaceutical Research*, 2015, 14: 27–34.
[24] V.M. Gun'ko, M.S. Vedamuthu, G.L. Henderson, et al. Mechanism and kinetics of hexamethyldisilazane reaction with a fumed silica surface. *Journal of Colloid and Interface Science*, 2000, 228: 157–170. https://doi.org/10.1006/jcis.2000.6934
[25] Z.H. Li, K.M. Su, B.W. Cheng, et al. Organically modified MCM-type material preparation and its usage in controlled amoxicillin delivery. *Journal of Colloid and Interface Science*, 2010, 342: 607–613. https://doi.org/10.1016/j.jcis.2009.10.073
[26] S.H. Han, W.G. Hou, J. Xu, et al. Synthesis of hollow spherical silica with MCM-41 mesoporous structure. *Colloid and Polymer Science*, 2004, 282: 1286–1291. https://doi.org/10.1007/s00396-004-1120-5
[27] I.W. Sayad, M.D.I. Mouzam, T. Imran. Simplistic spectroscopic method for determination of α-tocopheryl-acetate in bulk and formulated microemulsion. *International Journal of Pharmaceutical Research & Allied Sciences*, 2013, 2: 64–67.
[28] M. Brankovic, A. Zarubica, T. Andjelkovic, et al. Mesoporous silica (MCM-41): Synthesis/modification, characterization and removal of selected organic micro-pollutants from water. *Advanced Technologies*, 2017, 6: 50–57. https://doi.org/10.5937/savteh1701050b
[29] I. Kucuk, Z. Ahmad, M. Edirisinghe, et al. Utilization of microfluidic V-junction device to prepare surface itraconazole adsorbed nanospheres. *International Journal of Pharmaceutics*, 2014, 472: 339–346. https://doi.org/10.1016/j.ijpharm.2014.06.023
[30] T. Azaïs, G. Laurent, K. Panesar, et al. Implication of water molecules at the silica–ibuprofen interface in silica-based drug delivery systems obtained through incipient wetness impregnation. *The Journal of Physical Chemistry C*, 2017, 121: 26833–26839. https://doi.org/10.1021/acs.jpcc.7b08919
[31] S. Umar, M. Zahra, M. Akhter, et al. Novel surfactant stabilized PLGA cisplatin nanoparticles for drug delivery applications. *Turkish Journal of Chemistry*, 2021, 45: 1786–1795. https://doi.org/10.3906/kim-2105-41